

ELECTROWEAK MEASUREMENTS

CRISTINEL DIACONU

Centre de Physique des Particules de Marseille, IN2P3-CNRS, case 902, 163 Avenue de Luminy, Marseille, France
and Deutsches Elektronen Synchrotron, DESY, Notkestr. 85, 22607 Hamburg, Germany
E-mail: diaconu@cppm.in2p3.fr

The measurements of electroweak sector of the Standard Model are presented, including most recent results from LEP, Tevatron and HERA colliders. The robustness of the Standard Model is illustrated with the precision measurements, the electroweak fits and the comparisons to the results obtained from low energy experiments. The status of the measurements of the W boson properties and rare production processes involving weak bosons at colliders is examined, together with the measurements of the electroweak parameters in ep collisions.

1 Introduction

The Standard Model (SM) of the elementary particles has proven its robustness in the past decades due to extensive tests with increasing precision. In the present paper, the status of electroweak measurements in summer 2005 are presented. First, the precision measurements from LEP and SLD colliders will be summarised^a and the confrontation with the low energy experiments will be reviewed. Then production of weak bosons at LEP, Tevatron and HERA will be presented. The constraints obtained from an electroweak fit over DIS data will be described together with the latest measurements from polarized electron data at HERA. Finally, prospects for electroweak measurements at future colliders will be briefly reviewed.

2 The experimental facilities

The LEP collider stopped operation in 2000, after providing an integrated luminosity of more than 0.8 fb^{-1} accumulated by each of the four experiments (ALEPH, DELPHI, L3 and OPAL). The first stage (LEP I) running at Z peak was continued with a second pe-

riod (LEP II) with centre-of-mass energies up to 209, beyond the W pair production threshold. The physics at the Z peak was greatly enforced due to the polarised e^+e^- collisions programme at the SLC. The SLD detector recorded a data sample corresponding to an integrated luminosity of 14 pb^{-1} , with a luminosity weighted electron beam polarisation of 74%.

The Tevatron $p\bar{p}$ collider completed a first period (Run I) in 1996. After an upgrade, including the improvement of the two detectors CDF and D0, a second high luminosity period started in 2002. In summer 2005 the delivered integrated luminosity reached 1 fb^{-1} . The completion of the second part of the programme (Run II) is foreseen in 2009 with a goal of 4 to 8 fb^{-1} .

The unique $e^\pm p$ collider HERA is equipped with two detectors in collider mode H1 and ZEUS. After a first period with unpolarised collisions (HERA I, 1993–2000), in the new stage (HERA II) the collider provides both electron and positron–proton collisions with e^\pm beam polarisation of typically 40%. The HERA programme will end in 2007 with a delivered luminosity around 700 pb^{-1} .

The situation of the high energy colliders in the last 15 years was therefore a favourable one, with all three combinations of colliding beams e^+e^- , $p\bar{p}$ and ep . The most pre-

^aThe new averages of the W boson and top quark masses, made public¹ in July 2005 after the conference, are included in this paper together with the corresponding results of the electroweak fit.

cise testing of the weak interactions is done at e^+e^- colliders (LEP and SLC), where Z bosons are produced in the s -channel in a clean environment with sufficient luminosities. The hadronic collider (Tevatron) produces large samples of weak bosons and enables complementary studies at higher energies, including the measurement of the top quark properties. In ep collisions, the exchange of space-like electroweak bosons in the t channel leads to new experimental tests of the Standard Model. The high energy experiments are complemented by low energy measurements that test the electroweak theory with high precision far below the weak boson masses.

3 The precision measurements, the electroweak fits and comparisons with low energy data

3.1 The precision measurements from high energy experiments

The Standard Model is tested using a set of precision measurements at e^+e^- colliders close to the Z peak. Those measurements, which were finalised recently², include data from the LEP experiments and the SLD detector at the SLC.

The two fermion production is measured using the flavour tag of the final state (leptons ℓ and the b and the c quarks). More than 1000 measurements are used to extract a few observables that have simple relations to the fundamental parameters of the SM. The observables set include: the cross sections and its dependence on the \sqrt{s} (line shape given by Z mass m_Z , width Γ_Z and the hadronic pole cross section σ_{had}^0) and on final state flavour (partial widths $R_{\ell,b,c}$), the forward-backward asymmetries (A_{FB}), the left-right asymmetries (A_{LR} , measured for polarised beams or using the measured polarisation of the final state tau leptons). Moreover, the measured asymmetries are used in order to extract the asymmetry parameters that are

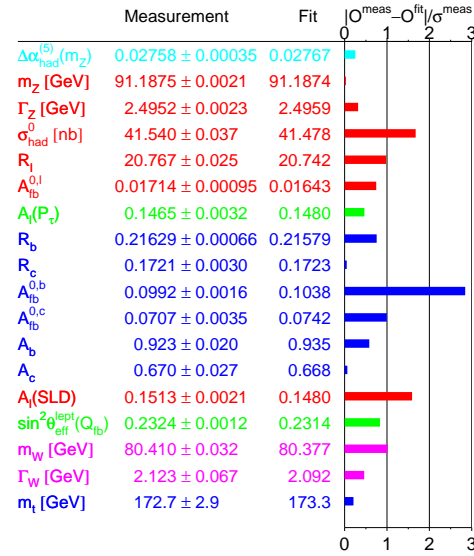


Figure 1. The observables of the SM electroweak test compared with the values predicted from the fit. The pulls are also graphically shown and display a consistent picture of the Standard Model. The largest deviation is found for A_{FB}^b , slightly below 3σ .

directly related to the ratio of axial and vector couplings $A_f = 2 \frac{g_V^f/g_A^f}{1+(g_V^f/g_A^f)^2}$. In the SM, $g_V^f/g_A^f = 1 - 4|Q_f| \sin^2\theta_{\text{eff}}^f$, where Q_f is the fermion charge and $\sin^2\theta_{\text{eff}}^f$ the effective weak mixing angle, defined as the weak mixing angle including the radiative corrections.

In order to relate the measurements to the fundamental constants of the SM, a simple parameter set is chosen. This includes the fine structure constant $\alpha(0)$, the strong coupling α_s , the mass of the Z boson m_Z and the Fermi constant G_F (related in practice to the W boson mass). All fermion masses are neglected except the top quark mass m_{top} . The Higgs boson mass m_{Higgs} plays a special role, due to its contribution to the radiative corrections. The observables are corrected for experimental effects and com-

pared to the predictions from the Standard Model $O(\alpha, \alpha_s, m_Z, G_F, m_{\text{top}}, m_{\text{Higgs}})$. The QCD and electroweak radiative corrections are needed to match the experimental accuracy. The observables are therefore calculated with a precision beyond two loops. The fermion couplings $g_{A,V}^f$ that enter most of the observables depend via the radiative correction logarithmically on m_{Higgs} and quadratically on m_{top} . This dependence allows the indirect determination of m_{Higgs} and m_{top} .

The running with energy of the electromagnetic coupling has to be taken into account in the radiative corrections. The running can be calculated analytically with high precision for the photon vacuum polarisation induced by the leptons and by the top quark. In contrast, the contribution due to the five light quark flavours $\Delta\alpha_{\text{had}}^{(5)}$ is non-perturbative and has to be deduced from the measured $e^+e^- \rightarrow \text{hadrons}$ cross section via the dispersion relations. The determination of $\Delta\alpha_{\text{had}}^{(5)}$ has been recently updated³ by including the new data from the ρ resonance measured by CMD-2⁴ and KLOE⁵. Despite a precision improvement by more than a factor of two in the ρ region, the impact on $\Delta\alpha_{\text{had}}^{(5)}$ precision is modest. QCD based assumptions may lead to an improved accuracy of the $\Delta\alpha_{\text{had}}^{(5)}$ extraction⁶. More precision measurements of hadron production in e^+e^- collisions at low energy (in preparation) can bring significant improvements for the consistency checks of the SM. In addition, the hadronic vacuum polarisation estimates based on this data are also of high interest for the $(g-2)_\mu$ measurement, for which a 2.7σ discrepancy between the observation and the theory persists^{6,7}.

The list of the measured observables, using latest input from the LEP and SLC experiments¹ is shown in figure 1. The fit of the observables in the SM framework is taken as a consistency check of the SM. The pulls of the observables plus the $\Delta\alpha_{\text{had}}^{(5)}$ are also shown in figure 1. The picture dis-

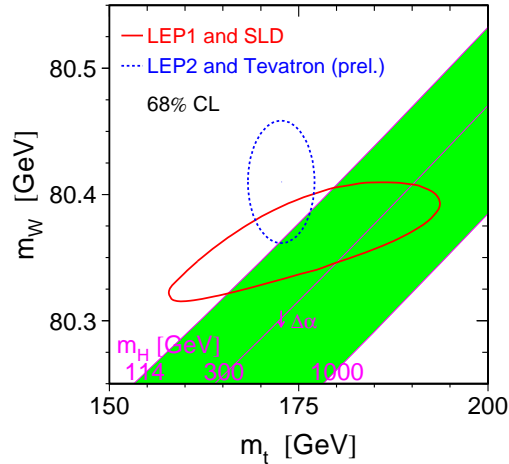


Figure 2. The comparison of the direct measurements and indirect determinations of the top quark and W boson masses. The band indicates the SM constraint from the G_F precise measurement for a range of Higgs masses. The confidence domain from the LEP1 and SLD data is compared with the direct measurement from LEP2 and Tevatron.

plays both the tremendous precision achieved by the electroweak tests and also the very good consistency of the SM. The most significant deviation, close to 3σ , is given by the forward-backward asymmetry of the b -quarks, A_{FB}^b . For this combined measurement, the individual values from various experiments and using different methods show very consistent results.

Subtracting the visible partial widths $\Gamma_{\ell,b,c}$ deduced from the individual cross section from the total Z width measured from the line shape, an invisible width can be deduced. Assuming that the invisible width is due to neutrinos with the same couplings as predicted by the SM, the number of neutrino flavours is determined to be $N_\nu = 2.9840 \pm 0.0082$, in agreement with the SM expectation of three fermion generations.

An important ingredient for the SM consistency check is the direct measurement of the top quark mass. Together with the direct

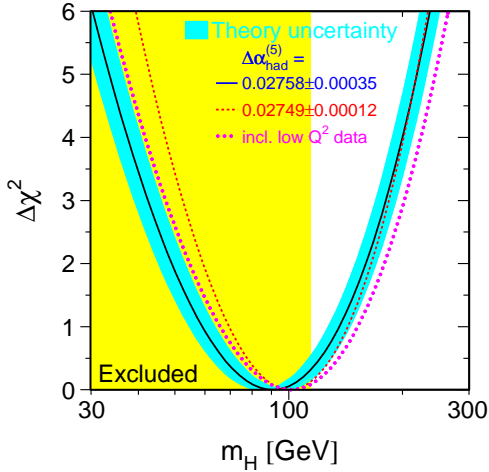


Figure 3. The χ^2 of the SM fit, including the measured top quark mass, as a function of the Higgs boson mass. The results using two different estimations of $\Delta\alpha_{\text{had}}^{(5)}$ are shown together with the χ^2 of the fit including the low energy data, described in the section 3.2. The theoretical error is indicated as a band.

determination of the W boson mass, to be discussed later, it constitutes a powerful test of the SM consistency. The new techniques and data samples from Run II improved the measurement of the top quark mass at Tevatron. The new average⁸, including recent measurement by the CDF and D0 collaborations is $m_{\text{top}} = 172.7 \pm 2.9$ GeV, a measurement which displays a dramatic improvement with respect to the previous error of 4.3 GeV (before the summer 2005). The comparison of the measured and fitted top and W masses is shown in figure 2. The direct and indirect determinations are in agreement and favour low m_{Higgs} . Due to close connections between the electroweak correction involving the top quark and Higgs boson, the precision of the top mass measurement is crucial for the indirect constraints on the Higgs mass. The new fit of the Higgs boson mass from the electroweak model is shown in figure 3. The new value of the fitted Higgs mass is $M_H = 91_{-32}^{+45}$ GeV with an upper limit within the SM

formalism $M_H < 186$ GeV at 95% CL. When the direct lower limit $M_{\text{Higgs}} > 114$ GeV is taken into account, the upper bound is found to be $M_H < 219$ GeV at 95% CL.

3.2 The electroweak precision measurements at lower energies

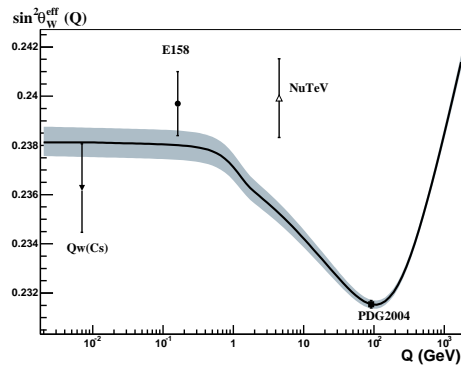


Figure 4. The measurements of effective mixing angle at various energies (Q) compared with the theoretical prediction.

Measurements of parity violation in the highly forbidden $6S-7S$ transition in Cs offer a way to test with high precision the SM¹¹. Due to its specific configuration with one valence electron above compact electronic shells, the theoretical calculation of the transition amplitude achieves 0.5% precision which allows the extraction with low ambiguities of the value for the nuclear weak charge¹². The weak charge of the nucleus depends linearly on the weak charges on the u and d quarks contained by the nucleons and interacting with the valence electron via γ/Z in the t -channel. The weak charge Q_w can therefore be written as a function of the effective weak mixing angle that can be measured in this way at very low (atomic-like) energies.

The weak interactions can be tested at low energies via parity violating reactions. Using the end of beam at the SLC, polarized electrons are scattered off unpolarised atomic electrons (E158 experiment). The polarised Moller scattering $e^-e^- \rightarrow e^-e^-$ offers

the opportunity to extract $\sin \theta_{\text{eff}}$ from cross section helicity asymmetry. This observable is related to the weak mixing angle that can be inferred with high precision¹⁰ at an energy of 160 MeV.

A classical way to access the weak sector at any energy is to measure neutrino induced processes. In the case of neutrino-nucleon scattering studied by the NuTeV experiment⁹, the ratio of neutral current to charged current cross sections $R_\nu = \sigma_{\text{CC}}/\sigma_{\text{NC}}$ is sensitive to the effective weak mixing angle, but subject to many systematic uncertainties related to the nucleon structure. Using both neutrino and anti-neutrino beams, the experimental results are combined using the Pachos–Wolfenstein method $R_- = (\sigma_{\text{NC}}^\nu - \sigma_{\text{NC}}^{\bar{\nu}})/(\sigma_{\text{CC}}^\nu - \sigma_{\text{CC}}^{\bar{\nu}})$, for which large cancellations of systematic errors are expected. This ratio accesses the effective weak mixing angle and is also sensitive to the neutrino and quark weak couplings. When SM couplings are assumed, the mixing angle measured by NuTeV is different from the SM prediction at 3.2σ level. Missing pieces in either the theoretical prediction or in the theory error associated to the measurement are still under investigation¹⁴.

The measurement of the effective weak mixing angle at high and low energy can be used to test the electroweak running¹³. The result is shown in figure 4. Good agreement is found with the theoretical prediction, except for the NuTeV measurement discussed above. Precise measurements at energies beyond M_Z , as expected at the next e^+e^- collider will test the predicted increase of $\sin^2 \theta_W^{\text{eff}}$ with energy.

3.3 The direct measurement of the running of α

The running of the electromagnetic coupling has been observed by the OPAL experiment using low angle Bhabba scattering $e^+e^- \rightarrow e^+e^-$ ¹⁵. The scattered electrons and

positrons are detected close to the beampipe by two finely segmented calorimeters that allow the measurement of the scattering angles. The transferred momentum t is therefore reconstructed and the variation of the cross section as a function of t can be measured. The cross section is directly proportional to the square of the electromagnetic coupling and inversely proportional to t^2 . The electromag-

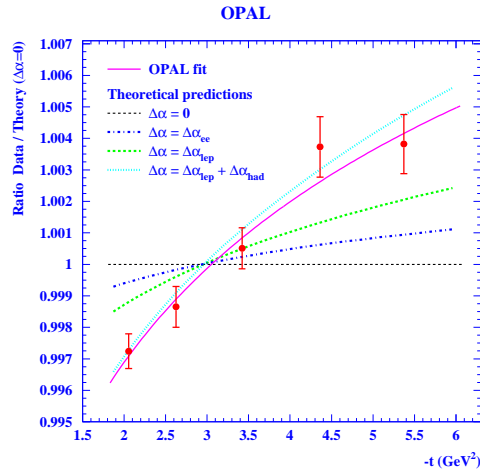


Figure 5. $|t|$ spectrum normalized to the theoretical prediction for a fixed coupling ($\Delta\alpha = 0$).

netic coupling is expected to run with the collision scale, given by t . The t spectrum normalised to the theoretical prediction for a fixed coupling is shown in figure 5. The difference of the measured event rates in t bins and the theoretical prediction for no α running shows a clear dependence on t . This evidence at 5σ level is compatible with the interpretation of $\alpha(t)$ running. When the pure electromagnetic running is taken into account in the theory, the remaining difference can be attributed to the hadronic component running that is in this way directly measured at 3σ level.

4 The weak bosons production and properties

4.1 The production of W and Z bosons

The weak boson production mechanisms at LEP2 and Tevatron provide a test of the SM. In addition, the weak boson samples can be used to study their decay properties and further constrain the Standard Model.

W pair production at LEP has been studied as a function of the centre-of-mass energy. The production cross-section variation with energy, flattens off at values around 15 pb, as expected from the SM, including the triple boson coupling ZWW . This behaviour is therefore directly related to the gauge structure of the Standard Model and constitutes an evidence for the non-abelian internal symmetry of the electroweak sector.

The W and Z bosons can be singly produced in $p\bar{p}$ collisions at Tevatron via the Drell-Yan process $q\bar{q} \rightarrow W$. The production cross section is sensitive to the parton distribution functions. From this point of view, the production mechanism is also a convenient test ground for QCD, since the radiative corrections apply only to colliding partons and decouple from the produced bosons. The W and Z production cross sections measured in $p\bar{p}$ collisions at Tevatron are measured using the leptonic decay channels in e , μ or τ . The results¹⁶ obtained from Run I ($\sqrt{s} = 1.8$ TeV) and Run II ($\sqrt{s} = 1.96$ TeV) are shown in figures 6 and show a good agreement with the NNLO calculation¹⁷.

4.2 The W mass, width and branching ratios

The W harvest is also used to study the W properties like the mass, the branching ratios and the width. The latest world average between the LEP and the Tevatron Run I measurements yields a $M_W = 80.410 \pm 0.032$ GeV. The direct measurement agrees with the indirect determination from the

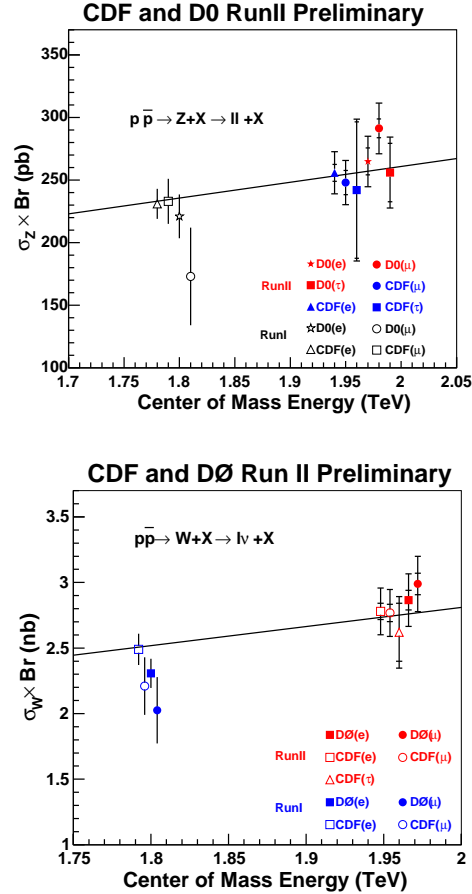


Figure 6. Measurements of the W and Z boson production cross section as a function of \sqrt{s} at Tevatron. Data from CDF and D0 experiments obtained from various channels are compared with the theoretical prediction based on a NNLO QCD calculation.

LEP and SLD electroweak fit, including the M_{top} constraint $M_W = 80.364 \pm 0.021$ GeV. The average include a recent final result published by the OPAL Collaboration¹⁸, for which a careful evaluation of the main systematical errors related to the colour reconnection and Bose-Einstein correlations together with an increased data sample allowed an improvement of the systematical error from 70 to 56 MeV. This final precision of one LEP experiment is already better than the one of the combined result from Tevatron Run I and UA2 measurements¹⁹ $M_W^{\text{runI+UA2}} =$

80.456 ± 0.059 GeV.

W pair production at LEP is a favourable configuration to measure W branching fractions. The decay to electron channel and to muon channel are found to be in very good agreement. However, the tau decay branching fraction is measured consistently by the four LEP experiments higher than the averaged electron and muon channel. This effect at 2.9σ is for the time being one of the largest deviations in the SM precision tests. Future measurements of $W \rightarrow \tau$ branching ratio are expected from Tevatron.

The W width can be measured directly from the invariant mass spectrum at LEP, where high precision can be achieved via a kinematic fit based on the energy-momentum conservation. At Tevatron, where only the leptonic channel is measurable, the transverse mass spectrum is sensitive to the W width in the tail at high mass. Finally, an indirect determination can be achieved exploiting the ratio of the W and Z cross section and using the precisely measured Z parameters and the theoretical prediction of the cross section ratios, for which most of the QCD uncertainties cancel out.

The present average of direct determination from LEP and Tevatron Run I is $\Gamma_W^{\text{direct}} = 2.123 \pm 0.067$, while the indirect determination from Run I data is 2.141 ± 0.057 . A recent direct determination²⁰ from Run II data by D0 still display large errors 2.011 ± 0.136 GeV, while an indirect determination using the cross section ratio measured by CDF already improves the Run I value 2.079 ± 0.041 GeV. The value obtained from the LEP1 and SLD electroweak fit is extremely precise 2.091 ± 0.002 GeV and in agreement with the direct and indirect determinations from LEP and Tevatron.

4.3 The A_{FB} from e^+e^- production at Tevatron.

The measurement of lepton pair production at Tevatron, produced via the Drell–Yan process $q\bar{q} \rightarrow \ell^+\ell^-$ provides complex information about both the proton structure and the electroweak effects in new energy domain. In particular, electron pair production can be used to measure the forward–backward asymmetry as a function of the pair mass. The result obtained by the D0 collaboration²¹ is shown in figure 7. The characteristic change of sign is observed around the Z mass, similar to the much more precise measurement from LEP. From the measured asymmetry, the effective weak mixing angle is extracted by CDF²² $\sin^2 \theta_W^{\text{eff}} = 0.2238 \pm 0.0050$, in good agreement with the value measured at LEP from the forward–backward asymmetry 0.2324 ± 0.0012 . At large invariant masses, the deviation from the SM prediction may indicate the production of a heavier neutral boson Z' , in case it has similar couplings to fermions as in the SM.

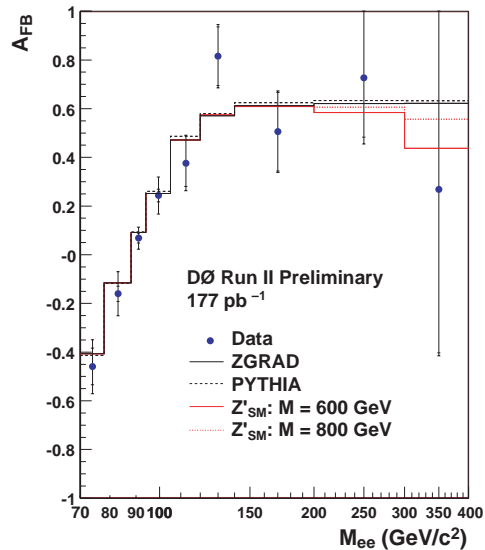


Figure 7. The A_{FB} as a function of the e^+e^- invariant mass measured at Tevatron.

Table 1. Summary of the results of searches for events with isolated leptons, missing transverse momentum and large hadronic transverse momentum p_T^X at HERA. The number of observed events is compared to the SM prediction. The W^\pm component is given in parentheses in percent. The statistical and systematic uncertainties added in quadrature are also indicated.

| obs./exp.(W) | | Electron | Muon | Tau ^{H1:105} pb ⁻¹ |
|--|------------------------|--|--|--|
| H1 211 pb ⁻¹ | Full sample | 25 / 20.4 ± 2.9 (68%) | 9 / 5.4 ± 1.1 (82%) | 5 / 5.8 ± 1.4 (15%) |
| | $p_T^X > 25\text{GeV}$ | 11 / 3.2 ± 0.6 (77%) | 6 / 3.2 ± 0.5 (81%) | 0 / 0.5 ± 0.1 (49%) |
| ZEUS 130 pb ⁻¹ 106 pb _{new} ⁻¹ | Full sample | 24 / 20.6 ^{+1.7} _{-4.6} (17%) | 12 / 11.9 ^{+0.6} _{-0.7} (16%) | 3 / 0.40 ^{+0.12} _{-0.13} (49%) |
| | $p_T^X > 25\text{GeV}$ | 2 / 2.90 ^{+0.59} _{-0.32} (45%) | 5 / 2.75 ^{+0.21} _{-0.21} (50%) | 2 / 0.20 ^{+0.05} _{-0.05} (49%) |
| | $p_T^X > 25\text{GeV}$ | 1 / 1.5 ± 0.2 (78%) | | |

4.4 Rare W and Z production processes

At LEP2, in contrast to W pair production, single boson production (W or Z) is a rare process with cross sections below 1 pb. The final state contains four fermions, with only one fermion pair consistent with the boson mass. The comparison to the Standard Model provides a test in a low density phase space region, where new phenomena can occur. The cross section is typically 0.6-0.9 pb for single W production and 0.5-0.6 pb for single Z production at $\sqrt{s} = 182 - 209$ GeV.

At Tevatron, where weak bosons are massively singly produced, boson pair occur with a much lower rate. The associated $W\gamma$ or $Z\gamma$ production processes, with the weak bosons decaying into leptons, have cross sections close to 20 pb and 5 pb respectively²³. The pair production of weak bosons is a particularly interesting process due to the spectacular final state and because it constitutes the main background for the search of the Higgs boson for $m_{\text{Higgs}} > 150$ GeV. While WW production has been measured^{24,25}, the search for WZ and ZZ production^{26,27} have not been successful with the present luminosity and upper limits around 13-15 pb at 95% CL have been calculated, for a total SM prediction of 5 pb.

The single W can also be produced in $e^\pm p$ collisions at HERA, with a cross section around 1 pb. The main production mechanism involves a fluctuation of photon emitted

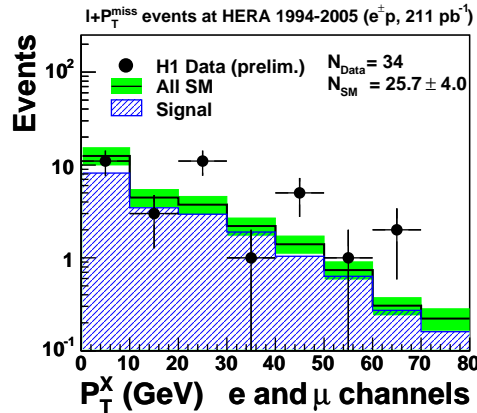


Figure 8. The transverse momentum of the hadronic system in events with isolated electrons or muons and missing P_T measured by the H1 experiment at HERA.

by the electron into a hadronic state, followed by the collision with the proton which leads to a qq' fusion into a W boson. In case of leptonic decay of the W , the final state consist of an high transverse momentum isolated lepton, missing transverse energy and possibly a low P_T hadronic system X . The H1 collaboration reported^{28,29} the observation of such events and measured the cross section as a function of the hadrons transverse momentum (P_T^X). While a good agreement is observed at low P_T^X , a few spectacular candidates are observed at large P_T^X . The events continue to be observed at HERA II³⁰ by the H1 Collaboration which has analysed a total

sample corresponding to an integrated luminosity of 211 pb^{-1} . The distribution of the transverse momentum of the hadronic system is shown in figure 8, where the excess of observed events at large P_T^X is visible.

The ZEUS collaboration has investigated their data with a different analysis strategy, with less purity for the SM W signal, the full HERA I data set and observes some events at large P_T^X , but no prominent excess above the SM prediction³¹. Recent modified analysis of the electron channel only, performed using a similar amount of data (but combining partial HERA I and II data sets) also do not support the H1 observation³². ZEUS collaboration observes events with tau leptons, missing transverse momentum and large hadronic transverse momentum, while no such event is observed by H1. The results are summarized in table 1. More incoming data will help to clarify this issue, which is at present one of the most intriguing results from HERA.

5 The measurement of the electroweak effects at HERA

5.1 Combined QCD/Electroweak fit of DIS data

The deep inelastic collisions at HERA are classically used to extract the proton structure information^{33,34}. More than 600 measurement points of the charged and neutral current double differential cross section $d\sigma^{CC,NC}/dx dQ^2$, where x is the proton momentum fraction carried by the struck quark and Q^2 is the boson virtuality, have been used together with other (fixed target) measurements to extract the parton distribution functions. Due to the high ep centre-of-mass energy (320 GeV), the proton is investigated down to scales of 10^{-18}m . The point-like nature of quarks is tested in the electroweak regime, where the proton is "flashed" with weak bosons. This experimental configuration allows to separate quark flavours within the proton and to improve the precision with

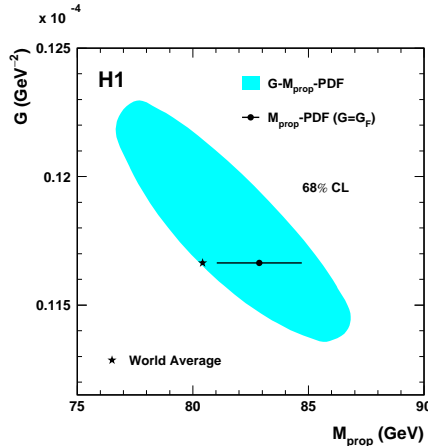


Figure 9. The allowed region at 65% CL in the plane (G_F, M_W^{prop}) obtained from the combined electroweak-QCD fit of the DIS data.

which the parton distribution functions are extracted. Conversely, the electroweak sector can be investigated using the knowledge of the proton structure.

Recently, a consistent approach has been adopted by the H1 Collaboration³⁵, performing a combined QCD-electroweak fit. The strategy is to leave free in the fit the EW parameters together with the parameterisation of the parton distribution functions.

An interesting result is related to the so-called propagator mass M_W^{prop} , that enters a model independent parameterisation of the CC cross section:

$$\frac{d^2\sigma_{CC}^{\pm}}{dx dQ^2} = \frac{G_F^2}{2\pi x} \left(\frac{M_W^2}{M_W^2 + Q^2} \right)^2 \tilde{\Phi}_{CC},$$

where G_F is the Fermi constant and $\tilde{\Phi}_{CC}$ is the reduced cross section that encapsulates the proton structure in terms of parton distribution functions. If the Fermi constant G_F and the propagator mass are left free in the fit, an allowed region in the (G_F, M_W^{prop}) plane can be measured. The result is shown in figure 9. By fixing G_F to the very precise experimental measurement, the propagator mass can be extracted

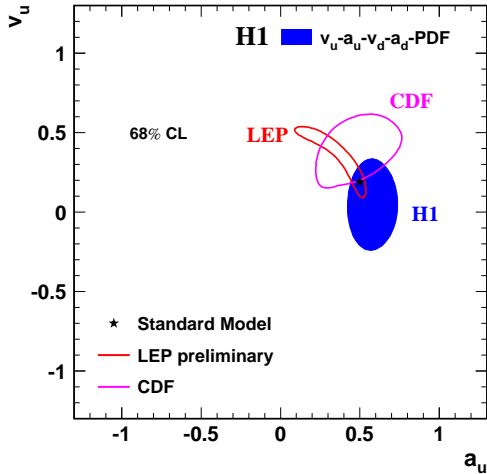


Figure 10. Axial and vector couplings of the u -quark measured from the combined electroweak-QCD fit at HERA and compared with measurements from LEP and Tevatron.

and amounts in this analysis to $M_W^{\text{PROP}} = 82.87 \pm 1.82(\text{exp.})_{-0.16}^{+0.30}(\text{model})$ GeV, in agreement with the direct measurements.

If the framework of SM model is assumed, the W mass can be considered as a parameter constrained by the SM relations and entering both the cross section and the higher order correction. In this fitting scheme, where M_W depends on the top and Higgs masses, the obtained value from DIS is $M_W = 80.709 \pm 0.205(\text{exp})_{-0.029}^{+0.048}(\text{mod}) \pm 0.025(\text{top}) \pm 0.033(\text{th}) - 0.084(\text{Higgs})$ GeV, in good agreement with other indirect determinations and with the world average. The fit value can be converted into an indirect $\sin^2 \theta_W$ determination using the relation $\sin^2 \theta_W = 1 - \frac{M_W^2}{M_Z^2}$, assumed in the on mass shell scheme. The result $\sin^2 \theta_W = 0.2151 \pm 0.0040_{\text{exp.}}_{-0.0011}^{+0.0019} |_{\text{th}}$, obtained for the first time in from $e^\pm p$ collisions, is in good agreement with the value of 0.2228 ± 0.0003 obtained from the measurements in e^+e^- collisions at LEP and SLC.

Due to the t -channel electron-quark scattering via Z bosons, the DIS cross sections at high Q^2 are sensitive to light quark ax-

ial (a_q) and vector (v_q) coupling to the Z . This dependence includes linear terms with significant weight in the cross section which allow to determine not only the value but also the sign of the couplings. In contrast, the measurements at the Z resonance (LEP1 and SLD) only access av or $a^2 + v^2$ combinations. Therefore there is an ambiguity between axial and vector couplings and only the relative sign can be determined. In addition, since the flavour separation for light quarks cannot be achieved experimentally, flavour universality assumptions have to be made. The Tevatron measurement²² of the Drell-Yan process allows to access the couplings at an energy beyond the Z mass resonance, where linear contributions are significant. The measurements of the u -quark couplings obtained at HERA, LEP and Tevatron are shown in figure 10. The data to be collected at Tevatron and HERA as well as the use of polarized e^\pm beams at HERA open interesting opportunities for the light quarks couplings measurements in the near future.

5.2 e^\pm collision with polarised lepton beam

The polarisation of the electron beam at HERA II allows a test of the parity non-conservation effects typical for the electroweak sector. The most prominent effect is predicted in the CC process, for which the cross section depends linearly on the e^\pm -beam polarisation: $\sigma^{e^\pm p}(P) = (1 \pm P)\sigma_{P=0}^{e^\pm p}$. The results^{36,37} obtained for the first time in $e^\pm p$ collisions are shown in figure 11. The expected linear dependence is confirmed and constitute supporting evidence for the V-A structure of charged currents in the Standard Model, a property already verified more than 25 years ago, by measuring the polarisation of positive muons produced from ν_μ -Fe scattering by the CHARM experiment³⁸.

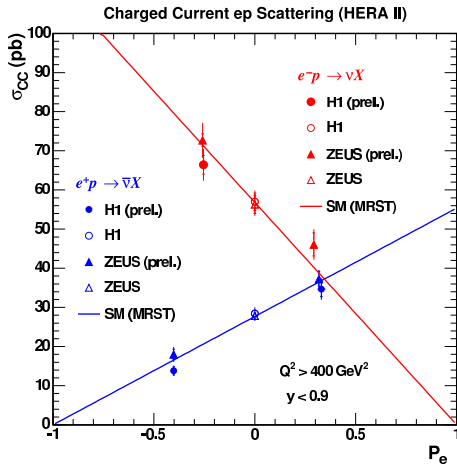


Figure 11. The dependence of the total CC cross section of the e^\pm -beam polarization at HERA.

6 Outlook

The present experimental activity towards electroweak measurements continues to provide increasing endurance tests for the Standard Model. The LEP analyses are final in many aspects and the results still play a key role in the present understanding of the electroweak symmetry breaking mechanism. The incoming data from Tevatron has good chance to take over in many aspects, especially concerning the weak boson properties, but also to extend the area of the measurements beyond LEP energies. At HERA, a consistent approach of the electroweak and QCD processes will certainly bring valuable information in the near future. The low energy measurements provide not only a cross check but also a solid testing ground for the electroweak sector, for which surprises are not excluded.

The future colliders will test the electroweak sector with high precision³⁹. At the LHC, the electroweak physics will mainly profit from the huge increase in the weak boson production cross-section. In the foreseen experimental condition the precision on the W mass measurement should approach

15 MeV while the top quark mass will be measured at 1 GeV level. The next e^+e^- linear collider will improve the precision on M_W to below 10 MeV while the top mass will be measured to 100 MeV. Similarly to the present situation, the precise measurements of the electroweak sector will allow to set indirect limits on the new physics, that might well be beyond the direct reach of the future colliders.

Acknowledgments

I would like to thank the following people for kind assistance during the preparation of this contribution: Max Klein, Martin Grunewald, Pippa Wells, Dmitri Denisov, Jan Timmermans, Bolek Pietrzyk, Emmanuelle Perez, Matthew Wing, Richard Hawkings, David Waters, Chris Hays and Dave South.

References

1. The LEP Collaborations, the LEP Electroweak Working Group, the SLD Electroweak, Heavy Flavour Groups, hep-ex/0412015, update for summer 2005 at <http://lepewwg.web.cern.ch/LEPEWWG>
2. The LEP Collaborations, the SLD Collaboration, the LEP Electroweak Working Group, the SLD Electroweak, Heavy Flavour Groups, hep-ex/0509008
3. H. Burkhardt and B. Pietrzyk, LAPP-EXP 2005-02
4. R. R. Akhmetshin *et al.* [CMD-2 Collaboration], Phys. Lett. B **578** (2004) 285 [hep-ex/0308008].
5. A. Aloisio *et al.* [KLOE Collaboration], Phys. Lett. B **606** (2005) 12 [hep-ex/0407048].
6. J. F. de Troconiz and F. J. Yndurain, Phys. Rev. D **71**, 073008 (2005) [hep-ph/0402285].
7. G. W. Bennett *et al.* [Muon g-2 Collaboration], Phys. Rev. Lett. **92**, 161802 (2004) [hep-ex/0401008].

8. [The CDF and D0 Collaborations], hep-ex/0507091.
9. G. P. Zeller *et al.* [NuTeV Collaboration], Phys. Rev. Lett. **88** 091802 (2002); [Erratum-ibid. 90 (2003) 239902] [hep-ex/0110059].
10. P. L. Anthony *et al.* [SLAC E158 Collaboration], hep-ex/0504049.
11. C.S. Wood *et al.*, Science **275** 1759 (1997)
12. J. S. M. Ginges and V. V. Flambaum, Phys. Rept. **397**, 63 (2004) [physics/0309054].
13. A. Czarnecki and W. J. Marciano, Int. J. Mod. Phys. A **15** (2000) 2365 [hep-ph/0003049].
14. J. T. Londergan, AIP Conf. Proc. **747**, 205 (2005).
15. G. Abbiendi *et al.* [OPAL Collaboration], hep-ex/0505072.
16. D. Acosta *et al.* [CDF II Collaboration], Phys. Rev. Lett. **94**, 091803 (2005) [hep-ex/0406078].
17. R. Hamberg, W. L. van Neerven and T. Matsuura, Nucl. Phys. B **359**, 343 (1991) [Erratum-ibid. B **644**, 403 (2002)].
18. G. Abbiendi [OPAL Collaboration], hep-ex/0508060.
19. V. M. Abazov *et al.* [CDF Collaboration], Phys. Rev. D **70**, 092008 (2004) [hep-ex/0311039].
20. Oliver Stelzer-Chilton, for the CDF and D0 Collaborations, hep-ex/0506016.
21. D0 Collaboration, Note 4757-CONF7, <http://www-d0.fnal.gov/Run2Physics/WWW/results/ew.htm>
22. D. Acosta *et al.* [CDF Collaboration], Phys. Rev. D **71**, 052002 (2005) [hep-ex/0411059].
23. D. Acosta *et al.* [CDF Collaboration], Phys. Rev. Lett. **94**, 041803 (2005) [hep-ex/0410008].
24. D. Acosta *et al.* [CDF Collaboration], Phys. Rev. Lett. **94**, 211801 (2005) [hep-ex/0501050].
25. V. M. Abazov *et al.* [D0 Collaboration], Phys. Rev. Lett. **94**, 151801 (2005) [hep-ex/0410066].
26. V. M. Abazov *et al.* [D0 Collaboration], Phys. Rev. Lett. **95**, 141802 (2005) [hep-ex/0504019].
27. D. Acosta *et al.* [CDF Collaboration], Phys. Rev. D **71**, 091105 (2005) [hep-ex/0501021].
28. C. Adloff *et al.* [H1 Collaboration], Eur. Phys. J. C **5**, 575 (1998) [hep-ex/9806009].
29. V. Andreev *et al.* [H1 Collaboration], Phys. Lett. B **561**, 241 (2003) [hep-ex/0301030].
30. V. Andreev *et al.* [H1 Collaboration], EPS2005 abstract 637, <http://www-h1.desy.de/h1/www/publications/htmlsplit/H1prelim-05-164.long.html>
31. S. Chekanov *et al.*, [ZEUS Collaboration] *Phys. Lett.* **B559** 153 (2003).
32. S. Chekanov *et al.* [ZEUS Collaboration], abstract 257, http://www-zeus.desy.de/physics/phch/conf/lp05_eps05/
33. C. Adloff *et al.* [H1 Collaboration], Eur. Phys. J. C **30**, 1 (2003) [hep-ex/0304003].
34. S. Chekanov *et al.* [ZEUS Collaboration], Phys. Rev. D **67**, 012007 (2003) [hep-ex/0208023].
35. A. Aktas *et al.* [H1 Collaboration], hep-ex/0507080.
36. V. Andreev *et al.* [H1 Collaboration], abstract 388, <http://www-h1.desy.de/h1/www/publications/htmlsplit/H1prelim-05-042.long.html>.
37. S. Chekanov *et al.* [ZEUS Collaboration], abstract 255, http://www-zeus.desy.de/physics/phch/conf/lp05_eps05/
38. M. Jonker *et al.*, Phys. Lett. B **86**, 229 (1979).
39. G. Weiglein *et al.* [LHC/LC Study Group], hep-ph/0410364